https://doi.org/10.3311/PPch.43653

Periodica Polytechnica Chemical Engineering

Catalytic and Non-Catalytic Pyrolysis of Pine Wood Residues: A Temperature-Based Study

Tarana Mammadova[1], Garanfil Ahmadova[2*], Nushaba Aliyeva[1], Elnura Mammadova[1]

[1] Institute of Petrochemical Processes, Azerbaijan National Academy of Sciences, 30 Khojaly Avenue, AZ1025 Baku, Azerbaijan
[2] Department of Chemical Engineering, Baku Higher Oil School, State Oil Company of the Azerbaijan Republic (SOCAR), Yeni Salyan Highway 3rd km, AZ1023 Baku, Azerbaijan
* Corresponding author, e-mail: qerenfil.ehmedova@bhos.edu.az

Received: 13 February 2026, Accepted: 15 June 2026, Published online: 19 August 2026

Abstract

Non-catalytic and magnetite-catalyzed pyrolysis of pine wood residues was systematically investigated in a fixed-bed reactor over the temperature range of 400–800 °C to elucidate the effects of temperature and magnetite catalysis on product distribution, composition, and energy quality. Calcined natural magnetite was employed as a low-cost catalyst to enhance cracking and reforming reactions during pyrolysis. Increasing temperature shifted product yields from liquids and char toward permanent gases in both systems; however, magnetite catalysis significantly intensified vapor-phase cracking and reforming reactions. Gas yields increased from 39.2–69.1 wt.% under catalytic conditions, compared to 18.2–54.8 wt.% for non-catalytic pyrolysis. Magnetite markedly reduced CO_2 formation and promoted syngas enrichment, with H_2, CO, and CH_4 contents reaching 19.1, 39.5, and 27.5 vol.% at 800 °C, respectively. As a result, the higher heating value of the gas increased from 16.4–28.9 MJ Nm^{-3}, exceeding that of the non-catalytic system (11.2–24.5 MJ Nm^{-3}). Compositional analysis showed that magnetite catalysis suppressed oxygenated compounds in the liquid phase *via* enhanced decarboxylation and decarbonylation, while promoting aromatization and polycyclic aromatic hydrocarbon formation; naphthalenes increased to 42.6 wt.% at 800 °C under catalytic conditions. Biochar produced in the presence of magnetite exhibited higher fixed carbon content, lower O/C and H/C ratios, and improved energy density, with a maximum higher heating value of 40.6 MJ kg^{-1} at 800 °C. These results demonstrate that calcined natural magnetite effectively tailors the biomass pyrolysis toward high-quality syngas, aromatics-rich liquids, and energy-dense biochar, supporting its application in integrated bioenergy systems.

Keywords

pine wood residues, catalytic pyrolysis, magnetite, temperature impact, higher heating value

1 Introduction

The depletion of fossil fuel reserves, coupled with socio-political conflicts arising from the concentrated extraction of these resources, has highlighted the urgent need for sustainable and renewable energy alternatives. Despite global efforts, fossil fuels such as coal, oil, and natural gas continue to dominate the world's energy supply, contributing significantly to greenhouse gas emissions and climate change [1, 2]. As a result, public awareness of the need to explore creative green alternatives and to sustainably produce and exploit renewable resources has increased. In this context, biomass has emerged as a promising renewable resource due to its abundance, carbon-rich composition, and potential for conversion into fuels, chemicals, and energy carriers, accounting for 10.4% of the world's primary energy supply and an impressive 77.4% of all renewable energy sources [3, 4]. Unlike fossil fuels, carbon released during biomass conversion originates from recently captured atmospheric CO_2, rendering biomass utilization near carbon-neutral and mitigating the greenhouse effect [5, 6].

Extensive research has been conducted on biomass conversion technologies, which can be broadly categorized into biological and thermochemical pathways. Biological conversion routes, relying on living organisms or enzymes, such as enzymatic lignin valorization, offer high product selectivity under mild operating conditions. However, these processes are often hindered by slow reaction kinetics, which limits their feasibility for large-scale industrial applications [7, 8]. In contrast, thermochemical conversion technologies – including gasification, torrefaction, and pyrolysis – have attracted considerable attention due to their

Cite this article as: Mammadova, T., Ahmadova, G., Aliyeva, N., Mammadova, E. "Catalytic and Non-Catalytic Pyrolysis of Pine Wood Residues: A Temperature-Based Study", Periodica Polytechnica Chemical Engineering, 2026. https://doi.org/10.3311/PPch.43653

operational flexibility, process robustness, and suitability for industrial-scale implementation [9, 10]. Among these, pyrolysis is particularly attractive as it enables the conversion of lignocellulosic biomass into three main product fractions: liquid bio-oil, solid biochar, and non-condensable gaseous products [11, 12]. These fractions can be further upgraded or utilized as renewable fuels and value-added chemicals [2, 13, 14]. The performance and product distribution of the pyrolysis process are strongly influenced by several factors, including biomass type, reactor configuration, operating temperature, and residence time [15–18]. Although bio-oil derived from pyrolysis demonstrates significant potential as a renewable energy carrier, its practical application is limited by high oxygen content and poor physicochemical stability, which adversely affect its energy density and long-term storage properties [19–21].

Catalytic pyrolysis represents an advanced alternative to conventional pyrolysis by enabling greater control over reaction pathways, thereby reducing the formation of undesirable byproducts and improving overall energy efficiency. In contrast to non-catalytic pyrolysis, catalytic pyrolysis suppresses the formation of complex mixtures rich in oxygenated compounds, thereby facilitating the production of higher-quality biofuels and renewable chemicals through more sustainable and economically viable routes [22–25]. Among the various catalysts investigated, zeolite-based materials – particularly ZSM-5 – have been extensively studied due to their shape-selective pore structures and strong Brønsted acid sites, which promote key reactions such as deoxygenation, aromatization, and olefin formation [24, 26–28]. Other zeolitic catalysts, including Y-zeolite, Beta-zeolite, mordenite, and ferrierite, exhibit distinct catalytic behaviors arising from differences in pore architecture and acid site distribution, resulting in varied product selectivity during biomass pyrolysis [29, 30].

In addition to zeolites, metal oxide catalysts such as magnesium oxide and titanium dioxide have demonstrated significant catalytic activity by facilitating deoxygenation reactions and enhancing hydrogen production [31–34]. Furthermore, natural mineral catalysts, including bentonite clay, as well as biochar-derived catalysts, have been explored due to their intrinsic alkali and alkaline earth metal content, which can contribute to catalytic activity [35, 36]. However, the catalytic performance of natural minerals and biochar is often limited by their heterogeneous composition, low specific surface area, and poorly defined active sites. These limitations result in reduced catalytic efficiency, lower selectivity, and potential issues related to catalyst stability and reproducibility [37, 38].

Although catalytic biomass pyrolysis has been widely investigated, most studies have focused on zeolites and synthetic metal oxides for improving bio-oil quality. Despite their effectiveness, these catalysts are often costly, susceptible to deactivation, and limited in scalability. Iron-based catalysts offer a promising alternative due to their abundance and favorable redox properties; however, available studies predominantly examine iron oxides in gasification or tar reforming systems, typically within narrow temperature ranges. The effect of natural magnetite on biomass pyrolysis, particularly its temperature-dependent influence on product yields and quality across gaseous, liquid, and solid fractions, remains insufficiently explored. Furthermore, existing research commonly addresses individual product streams independently, providing limited quantitative insight into the simultaneous effects of catalyst pretreatment on gas composition and heating value, liquid chemical composition, and biochar fuel properties. Integrated assessments linking temperature, magnetite catalysis, and overall product quality are scarce. To address these gaps, this study systematically compares non-catalytic and magnetite-catalyzed pyrolysis of pine wood residues over 400–800 °C using calcined natural magnetite (Fe_3O_4). By concurrently evaluating product yields and the physicochemical and energetic properties of all pyrolysis products, this work provides a quantitative basis for assessing the potential of magnetite as a low-cost catalyst for integrated bioenergy applications.

2 Materials and methods

2.1 Materials

In this research, Eldar pine (*Pinus eldarica*) wood residues were used as the biomass feedstock. This biomass was collected from pruning and wood-processing activities in the Absheron Peninsula, Azerbaijan. Prior to the experiment, the collected residues were dried at 100 °C for 20 h in a BINDER oven (FD 115, Germany), and subsequently ground into particles with a size of 1–2 mm.

Natural magnetite (Fe_3O_4) was utilized as the catalyst. The magnetite was sourced from the Dashkasan iron ore region of Azerbaijan. The raw material was crushed, milled, and washed with distilled water to remove surface impurities. After that, the washed catalyst was calcined at 550 °C for 2 h, and its crystal structure was generally preserved in the absence of oxygen; as a result, moisture and surface impurities were removed, and the thermal stability of magnetite was improved before catalytic pyrolysis. The specific surface area was evaluated to be 40 m^2/g from nitrogen adsorption-desorption isotherms recorded at −196 °C using an ASAP 2020 surface area and porosity

analyzer (Micromeritics, USA). This relatively high surface area indicates a porous structure and provides a large active surface for catalytic applications.

2.2 Physicochemical characterization

Proximate analysis of the dry sample, including the determination of volatile matter (VM), ash, and moisture content, was performed following ASTM E872-82(2019) [39], ASTM E1755-01(2020) [40] and ASTM E1756-01 [41] standards. Elemental compositions were measured in conformance with ASTM D5373-02 standard [42] using the Vario EL Cube elemental analyzer (model: Vario EL Cube, Elementar Analysensysteme GmbH, Langenselbold, Germany). The chemical composition was determined according to TAPPI standard methods: extractives (TAPPI T 204 cm-17 standard [43]), lignin (TAPPI/ANSI T 222 om-21 standard [44]), and cellulose (TAPPI T 203 cm-22 standard [45]), while hemicellulose content was calculated by difference.

2.3 Methods

Pyrolysis experiments were conducted in a laboratory-scale fixed-bed tubular reactor made of heat-resistant glass. The reactor was vertically positioned inside an electrically heated furnace equipped with a proportional–integral–derivative (PID) temperature controller. For each experiment, 350 g of biomass was used for non-catalytic runs, while for catalytic runs, a biomass–catalyst mixture was prepared. Calcined natural magnetite was added at a loading of 5 wt.% relative to the dry biomass amount of 350 g, corresponding to 17.5 g of catalyst per run. The catalyst and biomass (particle size 1–2 mm) were thoroughly homogenized prior to reactor loading to ensure uniform distribution. The catalyst was applied in an in-bed configuration, allowing primary pyrolysis and catalytic vapor upgrading to occur simultaneously within the same reaction zone. The schematic representation of the process is shown in Fig. 1.

Prior to the start of each experiment, the reactor was purged with high-purity nitrogen for a sufficient period to completely remove residual air and establish an oxygen-free atmosphere inside the system. The reactor temperature was increased from ambient temperature to the target pyrolysis temperatures at a constant heating rate of 25 °C min^{-1} under atmospheric pressure conditions, without the application of external pressure. The experiments were performed over a temperature range of approximately 400–800 °C to investigate the effect of temperature on product distribution. Once the target temperature was reached, it was maintained for a holding time of 1.5 h to allow complete thermal decomposition of the pine wood residues. The volatile products generated during pyrolysis exited the reactor and were directed into an ice-cooled condensation system, where condensable vapors were recovered as liquid products. The condensed liquid, consisting of bio-oil, water, and fine solid particles, was collected in a receiving flask. Non-condensable gases

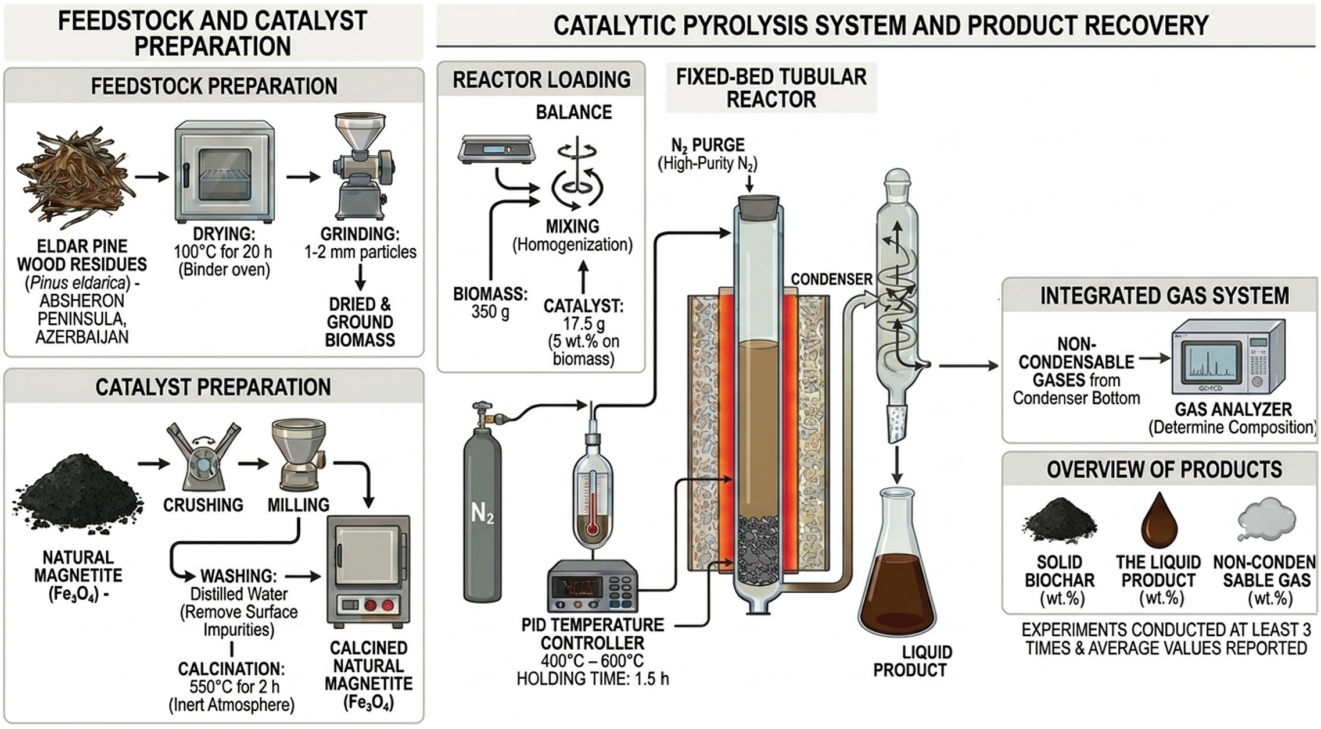

Fig. 1 Schematic representation of the process

were passed through a gas collection unit and analyzed with a gas analyzer to determine their composition. Solid biochar remained in the reactor after each run. After cooling to room temperature, the biochar and liquid products were carefully collected and weighed. Product yields of biochar, liquid, and gas were calculated as weight percentages relative to the initial dry biomass mass. Gas yield was determined by mass balance. All pyrolysis experiments were performed at least three times, and average values were reported to ensure the reproducibility and reliability of the results.

2.4 Characterization methods of pyrolysis products

2.4.1 Liquid product composition from gas chromatography–mass spectrometry

The composition of the bio-oil was determined using gas chromatography–mass spectrometry (GC/MS) analysis performed on an Agilent 8890 gas chromatograph coupled with an Agilent 5977C single quadrupole mass selective detector (Agilent Technologies Inc., Santa Clara, CA, USA). Before analysis, the particles were removed from the bio-oil samples using a 0.45 μm microfilter. The samples were then diluted with high-purity acetone and injected into the injection port (with an 80:1 split injection ratio) at a temperature of 230 °C. Pure helium was used as a carrier gas at a rate of 1.00 mL/min. The oven temperature was held at 300 °C for 20 min. The NIST mass spectrometry library was used to identify the composition of the bio-oil based on the respective peaks.

For the interpretation of GC/MS data, the term "relative content (rel. cont. %)" refers to the normalized peak area percentage of each identified compound or compound group with respect to the total integrated peak area of all detected components in the chromatogram. The relative content was calculated by dividing the individual peak area by the sum of all peak areas and multiplying by 100. Accordingly, the reported values represent semi-quantitative estimates of the compositional distribution of the liquid products. It should be noted that no external calibration or response factor correction was applied; therefore, the results are intended for comparative analysis of relative changes in chemical composition rather than absolute quantification.

2.4.2 Gas chromatography analysis of gas products

Non-condensable gases extracted from the reactor *via* a gas collector were subjected to gas chromatography (GC) analysis using a PE-G0-0300 PerkinElmer Autosystem XL GC apparatus (PerkinElmer, USA), equipped with a dual-channel, capillary injector, thermal conductivity detector TCD and flame ionization detector (FID) for the detection of components. The split ratio was set as 70:1, and high-purity helium was utilized as a carrier gas in split injection mode with a flow rate of 25 mL/min.

2.4.3 Biochar characterization

An elementary analyzer (Vario Macro cube, Germany) was utilized to determine the N, C, H and S elemental contents of biochar products, while the oxygen content was inferred from the variation relative to the whole sample, so it was determined by subtracting the sum of the percentages of hydrogen, carbon, nitrogen, and sulfur from 100. Proximate analyses of biochar were performed under ASTM D3172-13(2021)e1 [46], ASTM D3173/D3173M-25 [47], ASTM D3174-12(2018)e1 [48] and ASTM D3175-26 [49] standards to determine fixed carbon (FC), volatiles, ash, and water content.

2.4.4 Determination of higher heating value of biochar and gas products

The higher heating value (HHV) of pyrolysis products, including biochar and gas fraction, was determined using different approaches depending on the physical state of the product.

For solid biochar samples, HHV was measured experimentally using a Parr 6300 oxygen bomb calorimeter (Parr Instrument Company, USA), following standard calorimetric procedures in accordance with ASTM D5865/D5865M-19 standard [50]. Approximately 1 g of finely ground and oven-dried biochar sample was combusted in a high-purity oxygen atmosphere (≈30 bar), and the heat released during complete combustion was recorded.

The HHV of the gas mixture was calculated according to Eq. (1) [51–53], using the volumetric composition of combustible gas components determined by GC analysis:

$$\mathrm{HHV_{gas}} = \sum \left(y_i \times \mathrm{HHV}_i \right), \tag{1}$$

where y_i is the volumetric fraction (vol.%) of each gas component (H_2, CO, CH_4, C_2–C_3 hydrocarbons) on a dry gas basis, and HHV_i is the corresponding higher heating value of each component (MJ Nm^{-3}). Standard HHV values of pure gas components were taken from literature sources [51–53]. Carbon dioxide was excluded from the calculation due to its non-combustible nature.

3 Results and discussion

3.1 Physicochemical characteristics of pine wood residues

The physicochemical properties of pine wood residues (Table 1) indicate strong suitability for bio-oil–oriented

Table 1 Physicochemical characteristics of pine wood residues

Proximate analysis	wt.% (on dry basis)
Volatile matter	80.1
Moisture	3.1
Ash	0.5
Fixed carbon (based on difference)	16.3
VM/FC	4.9
Ultimate analysis	wt.% (on dry ash-free basis)
C	49.7
H	5.9
S	<0.02
N	0.8
O (based on difference)	43.6
C/H	8.42
Chemical analysis	wt.%
Hemicellulose	17.8
Cellulose	48.6
Lignin	26.5
Extractives	7.1
Energy content	MJ kg^{-1}
Higher heating value	19.8
Bulk density	kg/m^3
Ground pine wood residues	200.1

pyrolysis. Proximate analysis showed that pine wood residues have a moisture content of 3.1%, which is within the acceptable limit (< 10%) for thermochemical conversion [54]. Low moisture content is a key parameter for efficient pyrolysis, as elevated moisture levels increase energy consumption for water evaporation and negatively influence process efficiency and product yields. Consequently, biomass with a moisture content below 10% is considered suitable for achieving effective pyrolysis performance and improved product quality [54–56]. The high volatile matter content (80.1 wt.% on a dry basis) is the dominant factor governing product distribution, as rapid devolatilization under thermal treatment promotes the formation of condensable vapors and permanent gases [57, 58]. Consequently, biomass with such elevated volatile content favors higher bio-oil and gas yields, whereas feedstocks with lower volatile matter typically undergo enhanced carbonization, leading to increased biochar formation [59]. Pine wood biomass, with its low ash content of 0.5 wt.%, is ideal for pyrolysis, with most studies recommending ash levels below 5% [55, 60], as high ash levels can hinder heat transfer, promote undesirable secondary reactions, cause reactor fouling, and deactivate catalysts, ultimately reducing the yield and quality of bio-oil.

Ultimate analysis reveals high carbon (49.7 wt.%) and hydrogen (5.9 wt.%) contents with very low nitrogen (0.8 wt.%) and negligible sulfur contents (<0.02 wt.%), supporting efficient energy conversion with reduced emission potential, which is consistent with typical biomass compositions reported in previous studies [61, 62]. The relatively high oxygen content (43.58 wt.%) reflects the lignocellulosic nature of the biomass and contributes to the formation of oxygen-containing compounds in the liquid phase [56]. The chemical composition further explains the observed devolatilization behavior. The dominance of cellulose (48.6 wt.%) and hemicellulose (17.8 wt.%) favors volatile release and bio-oil formation [63], whereas lignin (26.5 wt.%) decomposes over a broader temperature range and contributes to both phenolic compounds and biochar [64]. The measured higher heating value of 19.8 MJ kg^{-1} confirms the energetic suitability of pine wood residues for thermochemical conversion. Overall, the high volatile matter, low ash content, and favorable lignocellulosic structure make pine wood residues an effective feedstock for bio-oil–focused pyrolysis applications.

3.2 Product distribution from non-catalytic and catalytic pyrolysis of pine wood residues

Fig. 2 illustrates the product yield distribution obtained from the non-catalytic pyrolysis of pine wood residues as a function of temperature, while Fig. 3 presents the corresponding results for Fe_3O_4-catalyzed pyrolysis. The distribution of pyrolysis products from pine wood residues was markedly affected by reaction temperature and the application of magnetite as a catalyst. In the non-catalytic system, increasing the temperature from 400 to 800 °C resulted in a continuous increase in gas yield from 18.2 to 54.8 wt.%, accompanied by a corresponding decrease in condensable

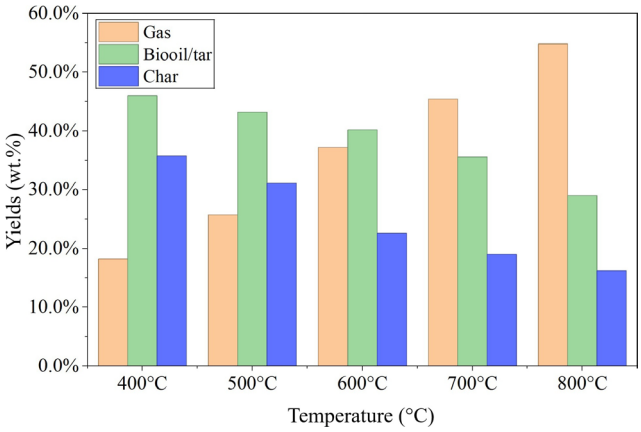

Fig. 2 Product yield distribution from the non-catalytic pyrolysis of pine wood biomass

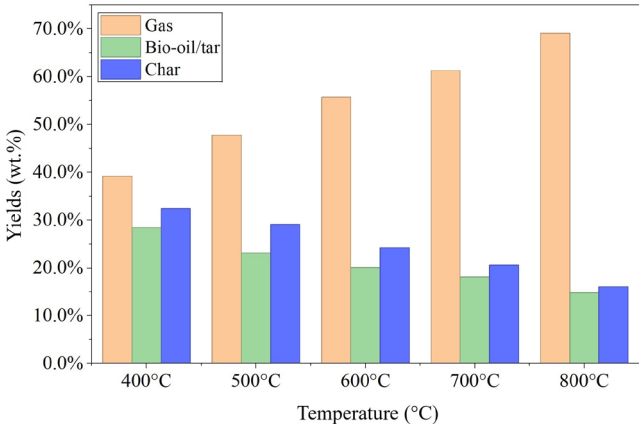

Fig. 3 Product yield distribution from the catalytic pyrolysis of pine wood biomass

liquid yield from 46.0 to 29.0 wt.% and char yield from 35.8 to 16.2 wt.%. This behavior is characteristic of enhanced devolatilization and intensified secondary thermal cracking of primary pyrolysis vapors at elevated temperatures, which promotes the conversion of condensable vapors into permanent gases and reduces liquid yields. Similar trends have been reported in previous studies, where increasing pyrolysis temperature enhanced secondary cracking reactions and significantly increased the formation of CO, H_2, CH_4, and other non-condensable gases while suppressing biooil and biochar production [65, 66].

In comparison, catalytic pyrolysis in the presence of Fe_3O_4 exhibited a pronounced shift toward gaseous products across the entire temperature range. Gas yields increased from 39.2 wt.% at 400 °C to 69.1 wt.% at 800 °C, consistently exceeding those obtained under non-catalytic conditions. Concurrently, condensable liquid yields were significantly suppressed, decreasing from 28.4 to 14.8 wt.%, which indicates the effective catalytic cracking and reforming of oxygen-containing vapor species. This observation is consistent with previous reports showing that metal-based catalysts promote deoxygenation, tar cracking, and reforming reactions, thereby increasing gas formation and reducing oxygenated liquid fractions [67–69]. Char yields under catalytic conditions were slightly lower than those observed in non-catalytic pyrolysis, suggesting that the catalyst predominantly influenced vapor-phase reactions rather than solid-phase decomposition [68]. Overall, the presence of magnetite as a catalyst significantly altered the pyrolysis reaction pathways by promoting secondary cracking and deoxygenation reactions, thereby favoring gas formation at the expense of liquid products. The catalytic effect became more pronounced at higher temperatures, demonstrating the synergistic role of thermal severity and catalytic activity in controlling product distribution during pine wood residue pyrolysis.

3.3 Effect of temperature and magnetite catalyst on gas composition and higher heating value

Figs. 4 and 5 present the GC analysis results of biogas produced from the non-catalytic and Fe_3O_4-catalyzed pyrolysis of pine wood residues, illustrating the strong influence of temperature and catalyst presence on gas composition. In non-catalytic pyrolysis, increasing the temperature from 400 to 800 °C shifted the gas composition from oxygen-rich species toward energy-rich components. Hydrogen and methane contents increased from 2.1 to 13.4 vol.% and from 4.6 to 19.2 vol.%, respectively, due to enhanced cracking of oxygen-containing intermediates. A similar pattern is consistent with previous findings reported by Lugovoy et al. [70], who observed that increasing temperature promotes secondary cracking reactions,

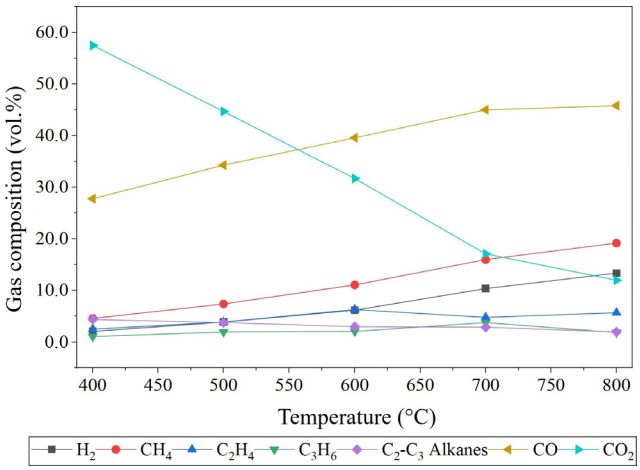

Fig. 4 Composition of biogas produced from non-catalytic pyrolysis of pine wood biomass

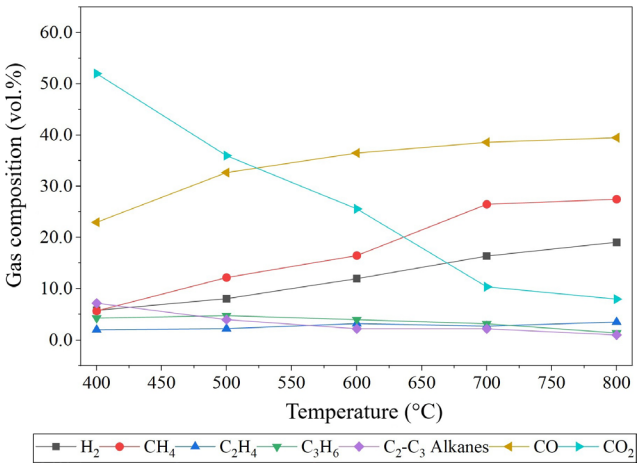

Fig. 5 Composition of biogas produced from the catalytic pyrolysis of pine wood biomass

resulting in higher concentrations of H_2 and light hydrocarbons. At low temperature, CO_2 dominated the gas phase (57.5 vol.% at 400 °C) and declined sharply to 12.0 vol.% at 800 °C, while CO increased from 27.8 to 45.8 vol.%, indicating progressive deoxygenation and activation of CO_2-consuming reactions. Similar behavior has been reported by Chai et al. [71], and Ismail et al. [72], who demonstrated that oxygen removal shifts from H_2O formation at low temperatures to CO and CO_2 evolution at higher temperatures, accompanied by increased CO production. C_2–C_3 hydrocarbons remained minor (<6 vol.%) and decreased at elevated temperatures because of secondary cracking.

In contrast, Fe_3O_4-catalyzed pyrolysis (Fig. 5) exhibits a distinctly different gas composition, highlighting the catalytic role of iron oxides. The catalyst significantly suppresses CO_2 formation across all temperatures, reducing its concentration to 8.0 vol.% at 800 °C, while simultaneously enhancing CO, H_2 and CH_4 production. Comparable trends have been reported for nickel-based catalysts, which are known to reduce CO_2 while increasing syngas components through reforming and cracking reactions [73, 74]. However, the catalytic behavior of Fe_3O_4 differs from conventional Ni- and zeolite-based catalysts due to its unique redox properties. Unlike Ni catalysts, which primarily act through metallic active sites for steam reforming, methanation, and tar cracking, Fe_3O_4 exhibits catalytic activity through the Fe^{3+}/Fe^{2+} redox cycle and oxygen transfer capacity, which strongly promotes deoxygenation reactions such as decarboxylation, decarbonylation, and the reverse water–gas shift reaction [75–78]. This explains the more pronounced suppression of CO_2 and the simultaneous enhancement of CO observed in the present study. At 800 °C, CO and H_2 reach 39.5 and 19.1 vol.%, respectively, indicating that magnetite formed *in situ* promotes endothermic reactions such as dry reforming, tar cracking, and the reverse water–gas shift reaction. The higher hydrogen content under catalytic conditions confirms the ability of iron oxides to facilitate C–C and C–H bond cleavage and accelerate secondary reforming reactions. Methane concentration is consistently higher in the catalyzed system, reaching 27.5 vol.% at 800 °C compared to 19.2 vol.% in the non-catalytic case, suggesting that iron oxide surfaces favor hydrogenation reactions at intermediate and high temperatures. Meanwhile, unsaturated hydrocarbons (C_2H_4 and C_3H_6) remain at low levels, implying their rapid conversion into smaller molecules over the catalyst surface.

These compositional changes are directly reflected in the HHV of the produced biogas (Fig. 6). HHV increases

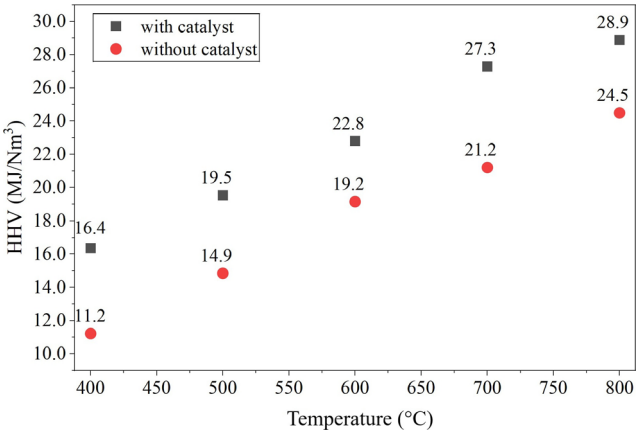

Fig. 6 HHV of biogas products from the noncatalytic and catalytic pyrolysis of pine wood biomass

monotonically with temperature for both systems due to the progressive enrichment of combustible gases (H_2, CO, and CH_4) and the reduction of inert CO_2. Non-catalytic biogas HHV increases from 11.2 MJ Nm^{-3} at 400 °C to 24.5 MJ Nm^{-3} at 800 °C, whereas Fe_3O_4-catalyzed pyrolysis yields significantly higher biogas HHVs, rising from 16.4 to 28.9 MJ Nm^{-3} over the same temperature range. The enhanced HHV under catalytic conditions is primarily attributed to increased methane and hydrogen concentrations and the suppression of CO_2 dilution effects.

Overall, increasing temperature shifts gas composition from CO_2-rich to syngas-rich mixtures, while the Fe_3O_4 catalyst substantially enhances syngas quality by promoting hydrogen and carbon monoxide formation and suppressing CO_2. These results demonstrate that the combined effect of high temperature and magnetite catalysis is effective for tailoring gas composition toward higher-value syngas suitable for downstream thermochemical applications, while also confirming Fe_3O_4 as a low-cost and environmentally favorable alternative to conventional metal-supported catalysts.

3.4 Effect of temperature and magnetite catalyst on liquid product composition

GC/MS analysis results shown in Tables 2 and 3 reveal that both pyrolysis temperature and Fe_3O_4 catalysis significantly influence the chemical composition of liquid products derived from pine wood biomass. In non-catalytic pyrolysis, oxygen-containing compounds (acids and esters, phenols, ketones, and alcohols) dominate at lower temperatures (400–500 °C), reflecting the primary thermal decomposition of cellulose and hemicellulose. As temperature increases, the relative abundance of acids and esters and ketones markedly decreases, indicating enhanced secondary cracking, decarboxylation, and

Table 2 GC/MS analysis results of the liquid products produced from the non-catalytic pyrolysis of pine wood biomass

Temperature of noncatalytic pyrolysis (rel. cont.%, based on GC/MS peak area)	400 °C	500 °C	600 °C	700 °C	800 °C
Acids and esters	23.9	17.5	13.4	10.6	7.8
Phenols	12.4	14.6	17	12.8	9.5
Ketones	19.4	22.5	13.8	10.3	9.2
Alcohols	4.0	3.6	2.5	2.0	1.4
Benzofurans	2.6	3.5	2.7	2.4	2.0
Other oxygenates	6.4	0.7	0.6	2.2	1.5
Naphthalenes	3.4	3.8	6.1	16.3	29.8
Phenanthrene	7.7	8.2	10.4	7.2	5.6
Acenaphthylene	2.4	3	4.2	3.5	3.4
Pyrene	4.2	8.4	10	7.4	5.0
1H-Phenalene	1.0	1.4	1.7	2.1	1.6
Fluoranthene	3.2	3.6	4.6	4.1	4.2
Fluorene + Anthracene	2.4	3.2	4.0	5.1	3.4
Other aromatics	7.0	6.0	9.0	14.0	15.6
Total	100	100	100	100	100

Table 3 GC/MS analysis results of the liquid products produced from the catalytic pyrolysis of pine wood biomass

Temperature of catalytic pyrolysis (rel.cont.%, based on GC/MS peak area)	400 °C	500 °C	600 °C	700 °C	800 °C
Acids and esters	13.7	6.3	3.7	1.9	1.0
Phenols	10.2	12.1	15.0	5.4	4.1
Ketones	10.3	15.6	6.8	5.3	4.2
Alcohols	2.8	2.2	1.7	1.2	0.5
Benzofurans	2.0	2.4	1.6	1.4	1.1
Other oxygenates	7.1	1.5	0.5	0.8	0.4
Naphthalenes	9.4	12.2	18.7	29.3	42.6
Phenanthrene	9.5	10.4	13.2	16.6	8.1
Acenaphthylene	4.3	5.7	6.1	7.0	7.2
Pyrene	8.5	9.6	12.4	10.3	9.0
1H-Phenalene	2.0	2.6	3.1	3.6	2.5
Fluoranthene	5.6	6.3	6.1	5.8	5.0
Fluorene + Anthracene	4.6	4.9	5.1	5.4	5.7
Other aromatics	10.0	8.2	6.0	6.0	8.6
Total	100	100	100	100	100

dehydration reactions. These findings are consistent with previous studies on lignocellulosic biomass (e.g., beech wood and corn stover), where oxygenated compounds decrease significantly above ~500–600 °C due to enhanced secondary cracking and deoxygenation reactions [65, 79]. In those studies, acids and esters showed reductions of comparable magnitude, supporting the trend observed in this study. Conversely, increasing temperature strongly promotes aromatic hydrocarbon formation. In the non-catalytic system, monocyclic and polycyclic aromatic hydrocarbons (PAHs) increase substantially above 600 °C, with naphthalenes rising sharply from 6.1% at 600 °C to 29.8% at 800 °C. This trend confirms that high temperatures favor aromatization, ring condensation, and polymerization of volatile intermediates into PAH-2 and PAH-3 structures, as reported in the literature [80].

The introduction of magnetite catalysts intensifies these compositional shifts. Compared to non-catalytic pyrolysis, Fe_3O_4 significantly suppresses oxygen-containing compounds across all temperatures. At 800 °C, acids and esters are reduced to only 1% under catalytic conditions, compared to 7.8% in the non-catalytic case. This indicates that the catalyst effectively promotes deoxygenation pathways such as decarboxylation and decarbonylation, improving the chemical stability of the liquid product. Similar deoxygenation behavior has been reported for ZSM-5 and HZSM-5 catalysts, although those systems typically achieve oxygen removal *via* Brønsted acid-catalyzed pathways. In contrast, the Fe_3O_4 catalyst used in this study promotes deoxygenation primarily through metal oxide surface reactions, suggesting a different dominant mechanism despite leading to comparable reductions in oxygenated species [22, 81–83]. Simultaneously, the magnetite catalyst markedly enhances aromatic hydrocarbon production. Naphthalene content reaches 42.6% at 800 °C under catalytic conditions, substantially higher than that obtained without a catalyst. This catalytic effect is attributed to iron-oxide-assisted cracking, cyclization, and aromatization reactions, which favor PAH growth and condensation. The increased formation of multi-ring aromatics such as phenanthrene, pyrene, and fluoranthene further confirms the role of the catalyst in promoting secondary vapor-phase reactions. This observation is consistent with previous reports indicating that iron-based catalysts enhance PAH growth *via* condensation and aromatization pathways. However, compared to zeolite catalysts such as HZSM-5, which typically favor monocyclic aromatics due to shape-selective pore structures, Fe_3O_4 in this study promotes the formation of heavier multi-ring PAHs, suggesting a shift toward polymerization-dominated reaction pathways [84, 85].

Overall, temperature governs the transition from oxygenated to aromatic-rich liquids, while Fe_3O_4 catalysis accelerates this transformation by selectively reducing

oxygenates and enhancing PAH formation. These results demonstrate that Fe_3O_4-catalyzed high-temperature pyrolysis is an effective strategy for producing aromatics-rich pyrolysis oils with reduced oxygen content.

3.5 Effect of temperature and magnetite catalyst on biochar composition and higher heating value

Pyrolysis temperature markedly influenced the compositional evolution and energy properties of pine wood biochar under both non-catalytic and Fe_3O_4-catalyzed conditions, and the results are demonstrated in Tables 4 and 5, respectively. A clear increase in fixed carbon was observed with increasing temperature, indicating enhanced carbonization and greater thermal stability of the solid carbon matrix. Under non-catalytic conditions, fixed carbon content increased from 69.7 wt.% at 400 °C to 92.1 wt.% at 800 °C. In the presence of Fe_3O_4 catalyst, the increase was even more pronounced, rising from 75.3 wt.% at 400 °C to 94.2 wt.% at 800 °C. These results demonstrate that higher pyrolysis temperatures significantly promote the transformation of pine wood biomass into a highly carbonized and energy-dense biochar. Similar increases in fixed carbon content with temperature were reported by Nurhadi et al. [86], where fixed carbon increased from 26.35% to 65.66% as pyrolysis temperature increased from 300 to 600 °C, and by Nath et al. [87], who observed an increase from 31.60% to 55.49% between 300 and 600 °C. The trend observed in the present study confirms that pine wood residues follow the same thermochemical transformation pattern, with higher temperatures favoring the formation of a more carbon-rich and thermally stable biochar structure. The elevated fixed carbon content observed in pine wood biochar can be primarily attributed to the inherent lignocellulosic composition of pine wood, particularly its relatively high lignin content and low ash fraction. Lignin is the most thermally stable component of biomass and decomposes over a broader temperature range than cellulose and hemicellulose, thereby contributing significantly to char formation [88–91]. During pyrolysis, cellulose and hemicellulose decompose preferentially at lower temperatures, releasing volatile compounds such as CO, CO_2, CH_4, and light oxygenated organics, while lignin undergoes gradual condensation and repolymerization reactions that favor the formation of stable polyaromatic carbon structures [92]. As a result, woody biomass such as pine wood generally produces biochar with higher fixed carbon content compared to agricultural residues and herbaceous feedstocks.

This was accompanied by increasing carbon content and declining hydrogen and oxygen concentrations, resulting in progressively lower H/C and O/C ratios and indicating enhanced aromatization and structural ordering of the carbon matrix. These temperature-driven changes directly improved the biochar's energy density. The progressive removal of oxygenated functional groups through dehydration and decarboxylation reduced biochar polarity and increased aromatic carbon concentration, yielding a steady increase in HHV of biochar product, which reached 37.9 MJ kg^{-1} for non-catalytic biochar at 800 °C.

Table 4 Physicochemical properties of biochar products produced from the non-catalytic pyrolysis of pine wood biomass

Pyrolysis temperature	Proximate analysis				Elemental analysis							HHV (MJ kg^{-1})
	Moisture (wt.%)	Volatile matter (wt.%)	Fixed carbon (wt.%)	Ash content (wt.%)	C content (wt.%)	H content (wt.%)	O content (wt.%)	N content (wt.%)	S content (wt.%)	O/C	H/C	
400	1.6	27.7	69.7	1.1	72.1	4.3	23.5	0.26	0.07	0.33	0.06	29.5
500	1.4	19.6	77.6	1.4	80.6	3.1	16.2	0.38	0.07	0.20	0.04	32.9
600	1.3	14.7	82.5	1.6	86.7	2.4	10.8	0.49	0.08	0.12	0.03	34.6
700	1.2	9.6	87.3	1.9	88.8	1.6	9.5	0.56	0.08	0.11	0.02	36.2
800	1.3	4.5	92.1	2.1	92.3	1.2	6.4	0.60	0.08	0.07	0.01	37.9

Table 5 Physicochemical properties of biochar products produced from the catalytic pyrolysis of pine wood biomass

Pyrolysis temperature	Proximate analysis				Elemental analysis							HHV (MJ kg^{-1})
	Moisture (wt.%)	Volatile matter (wt.%)	Fixed carbon (wt.%)	Ash content (wt.%)	C content (wt.%)	H content (wt.%)	O content (wt.%)	N content (wt.%)	S content (wt.%)	O/C	H/C	
400	1.3	22.1	75.3	1.3	75.7	3.8	20.4	0.30	0.07	0.27	0.05	31.8
500	1.2	14.3	82.9	1.6	82.5	2.5	14.9	0.40	0.08	0.18	0.03	34.9
600	1.1	9.4	87.6	1.9	89.4	2.0	8.5	0.49	0.08	0.10	0.02	36.7
700	1.1	5.2	91.6	2.1	91.6	1.4	6.9	0.57	0.09	0.08	0.02	38.8
800	1.0	2.4	94.2	2.4	94.4	0.9	4.6	0.62	0.09	0.05	0.01	40.6

The addition of a magnetite catalyst further intensified carbonization and deoxygenation across all temperatures. Catalytic biochars consistently exhibited higher fixed carbon contents, lower oxygen levels, and reduced O/C and H/C ratios compared with non-catalytic samples, reflecting more efficient secondary cracking and redox-assisted deoxygenation. As a result, HHV values of biochar samples were systematically higher in the presence of the catalyst, reaching 36.7 MJ kg^{-1} at 600 °C and a maximum of 40.6 MJ kg^{-1} at 800 °C. Notably, the catalyst enabled the production of high-energy biochar at lower temperatures, indicating reduced thermal severity requirements. Despite a slight increase in ash content, the combined influence of elevated temperature and magnetite catalysis yielded biochar with more coal-like elemental characteristics and improved energy density.

4 Conclusion

This study systematically investigated the effects of temperature (400–800 °C) and calcined natural magnetite (Fe_3O_4) on the distribution, composition, and energy properties of products obtained from the pyrolysis of pine wood residues. The results confirm that both temperature and catalyst presence exert a decisive influence on product yield and quality.

For gaseous products, the optimal performance was achieved at 800 °C under catalytic conditions, yielding the highest gas fraction (69.1 wt.%) with a syngas-rich composition (H_2: 19.1 vol.%, CO: 39.5 vol.%, CH_4: 27.5 vol.%) and a maximum HHV of 28.9 MJ Nm^{-3}, indicating superior fuel quality and reduced CO_2 content. For liquid products, the most favorable composition was also obtained at 800 °C with Fe_3O_4, where oxygenated compounds were significantly suppressed (acids and esters ~1%) and aromatic hydrocarbons were maximized, with naphthalenes reaching 42.6 wt.%, demonstrating effective catalytic deoxygenation and aromatization. For biochar, the best properties were observed at 800 °C under catalytic conditions, with a maximum fixed carbon content of 94.2 wt.%, a low O/C ratio (0.05), and the highest HHV of 40.6 MJ kg^{-1}, indicating the formation of a highly carbonized and energy-dense solid fuel. Additionally, catalytic pyrolysis at intermediate temperatures (e.g., 600 °C) produced biochar with relatively high HHV (36.7 MJ kg^{-1}), suggesting improved energy efficiency at lower thermal severity.

Overall, 800 °C with Fe_3O_4 represents the optimal condition for maximizing product quality across all phases, while intermediate temperatures provide a balance between energy efficiency and product performance.

The key novelty of this work lies in the integrated, temperature-dependent evaluation of all three product streams (gas, liquid, and solid) under magnetite catalysis, providing a comprehensive understanding of how Fe_3O_4 influences pyrolysis pathways. Unlike previous studies that focus on individual products, this research establishes a direct correlation between operating conditions and multi-phase product optimization. These results demonstrate that calcined natural magnetite is an effective, low-cost catalyst for tailoring biomass pyrolysis toward high-value energy carriers, offering strong potential for application in integrated bioenergy and biorefinery systems.

References

[1] Abbasov, V. M., Mammadova, T. A., Ahmadova, G. J., Latifova, T. S., Aliyeva, N. M. "Investigation of pyrolysis byproducts derived from beech wood residues", Processes of Petrochemistry and Oil Refining, 25(3), pp. 675–684, 2024. https://doi.org/10.62972/1726-4685.2024.3.675

[2] Carrasco Díaz, A., Abdelouahed, L., Brodu, N., Montes-Jiménez, V., Taouk, B. "Upgrading of Pyrolysis Bio-Oil by Catalytic Hydrodeoxygenation, a Review Focused on Catalysts, Model Molecules, Deactivation, and Reaction Routes", Molecules, 29(18), 4325, 2024. https://doi.org/10.3390/molecules29184325

[3] Sun, Y. "Technology Research and Development Prospects of Biofuels", Journal of Education and Educational Research, 7(1), pp. 11–15, 2024. https://doi.org/10.54097/ks2m1h72

[4] Yang, Y., Brammer, J. G., Wright, D. G., Scott, J. A., Serrano, C., Bridgwater, A. V. "Combined heat and power from the intermediate pyrolysis of biomass materials: performance, economics and environmental impact", Applied Energy, 191, pp. 639–652, 2017. https://doi.org/10.1016/j.apenergy.2017.02.004

[5] Chen, W.-H., Lee, K. T., Ong, H. C. "Biofuel and Bioenergy Technology", Energies, 12(2), 290, 2019. https://doi.org/10.3390/en12020290

[6] Raud, M., Kikas, T., Sippula, O., Shurpali, N. J. "Potentials and challenges in lignocellulosic biofuel production technology", Renewable and Sustainable Energy Reviews, 111, pp. 44–56, 2019. https://doi.org/10.1016/j.rser.2019.05.020

[7] Elgarahy, A. M., Hammad, A., El-Sherif, D. M., Abouzid, M., Gaballah, M. S., Elwakeel, K. Z. "Thermochemical conversion strategies of biomass to biofuels, techno-economic and bibliometric analysis: A conceptual review", Journal of Environmental Chemical Engineering, 9(6), 106503, 2021. https://doi.org/10.1016/j.jece.2021.106503

[8] Schmitt, N., Apfelbacher, A., Jäger, N., Daschner, R., Stenzel, F., Hornung, A. "Thermo-chemical conversion of biomass and upgrading to biofuel: The Thermo-Catalytic Reforming process – A review", Biofuels, Bioproducts and Biorefining, 13(3), pp. 822–837, 2019. https://doi.org/10.1002/bbb.1980

[9] K N, Y., T, P. D., P, S., S, K., R, Y. K., Varjani, S., AdishKumar, S., Kumar, G., J, R. B. "Lignocellulosic biomass-based pyrolysis: A comprehensive review", Chemosphere, 286, 131824, 2022. https://doi.org/10.1016/j.chemosphere.2021.131824

[10] Tyagi, U., Anand, N., Jain, A. K. "Pyrolysis of forestry biomass and its effect over bed arrangements and thickness for the production of fuels", Bioresource Technology Reports, 20, 101247, 2022. https://doi.org/10.1016/j.biteb.2022.101247

[11] Afraz, M., Muhammad, F., Nisar, J., Shah, A., Munir, S., Ali, G., Ahmad, A. "Production of value added products from biomass waste by pyrolysis: An updated review", Waste Management Bulletin, 1(4), pp. 30–40, 2024. https://doi.org/10.1016/j.wmb.2023.08.004

[12] Du, J., Gao, L., Yang, Y., Chen, G., Guo, S., Omran, M., Chen, J., Ruan, R. "Study on thermochemical characteristics properties and pyrolysis kinetics of the mixtures of waste corn stalk and pyrolusite", Bioresource Technology, 324, 124660, 2021. https://doi.org/10.1016/j.biortech.2020.124660

[13] Kumar, V., Sharma, N., Abdelaal, A. S., Chakraborty, P., Thomas, J., Duhan, L., Pasrija, R., Dogra, S., Jayaraj, I. "Bio-oil production and catalytic upgrade to value added product: A review on recent technologies", Journal of the Energy Institute, 118, 101880, 2025. https://doi.org/10.1016/j.joei.2024.101880

[14] Maity, P., Khande, A., Majumdar, S., Sharma, A., Thota, C. "Chapter 11 - Hydroprocessing and catalytic upgrading of bio-crude for clean transportation fuels", In: Nanda, S., Mondal, P. (eds.) Next-Generation Biofuels, Elsevier, 2026, pp. 235–260. ISBN 978-0-443-27564-7 https://doi.org/10.1016/B978-0-443-27564-7.00009-0

[15] Bhaskar, T., Pandey, A. "Chapter 1 - Advances in Thermochemical Conversion of Biomass—Introduction", In: Pandey, A., Bhaskar, T., Stöcker, M., Sukumaran, R. K. (eds.) Recent Advances in Thermochemical Conversion of Biomass, Elsevier, 2015, pp. 3–30. ISBN 978-0-444-63289-0 https://doi.org/10.1016/B978-0-444-63289-0.00001-6

[16] Jerzak, W., Acha, E., Li, B. "Comprehensive Review of Biomass Pyrolysis: Conventional and Advanced Technologies, Reactor Designs, Product Compositions and Yields, and Techno-Economic Analysis", Energies, 17(20), 5082, 2024. https://doi.org/10.3390/en17205082

[17] Ridwan, A., Istana, B., Abdurrahman, R., Israyandi, Aprio, T. "Investigating Bio-Oil Yield from Co-pyrolysis of Mixed Medical Waste and Biomass under Varying Temperature and Residence Time", International Journal of Automotive and Mechanical Engineering, 22(2), pp. 12293–12303, 2025. https://doi.org/10.15282/ijame.22.2.2025.4.0941

[18] Tripathi, M., Sahu, J. N., Ganesan, P. "Effect of process parameters on production of biochar from biomass waste through pyrolysis: A review", Renewable and Sustainable Energy Reviews, 55, pp. 467–481, 2016. https://doi.org/10.1016/j.rser.2015.10.122

[19] Imran, A., Bramer, E. A., Seshan, K., Brem, G. "Catalytic Flash Pyrolysis of Biomass Using Different Types of Zeolite and Online Vapor Fractionation", Energies, 9(3), 187, 2016. https://doi.org/10.3390/en9030187

[20] Lawan Muhammad, U., Shamsuddin, I. M., Danjuma, A., Musawa, R. S., Hafsat Dembo, U. "Biofuels as the Starring Substitute to Fossil Fuels", Petroleum Science and Engineering, 2(1), pp. 44–49, 2018. https://doi.org/10.11648/j.pse.20180201.17

[21] Moraes, M. S. A., Tomasini, D., da Silva, J. M., Machado, M. E., Krause, L. C., Zini, C. A., Jacques, R. A., Caramão, E. B. "Chromatographic Methods Applied to the Characterization of Bio-Oil from the Pyrolysis of Agro-Industrial Biomasses", In: Jacob-Lopes, E., Queiroz Zepka, L. (eds.) Frontiers in Bioenergy and Biofuels, IntechOpen, 2017, pp. 71–116. ISBN 978-953-51-2892-2 https://doi.org/10.5772/66326

[22] Bianasari, A. A., Le, M. T., Bakar, M. S. A., Saepurahman, Mansur, D., Md Ja'afar, F. H., Cheok, Q., Azad, A. K. "Phenol-rich bio-oil synthesis via single and dual metal-oxide/zeolite catalysts in biomass catalytic pyrolysis: Comparison of Y_2O_3/ZSM-5 and MgO/Y_2O_3/ZSM-5", Biomass and Bioenergy, 205, 108565, 2026. https://doi.org/10.1016/j.biombioe.2025.108565

[23] Kim, J. Y., Yoo, Y., Lee, D.-J., Park, J., Kwon, D. Y., Kim, K. Y., Cho, M., Kim, J.-J., Kwon, E. E. "Catalytic pyrolysis of three industrial fungal biomass to enhance syngas production", Fuel, 405, 136748, 2026. https://doi.org/10.1016/j.fuel.2025.136748

[24] Mishra, R. K., Chistie, S. M., Naika, S. U., Mohanty, K. "Catalytic pyrolysis of biomass over zeolites for bio-oil and chemical production: A review on their structure, porosity and acidity co-relation", Bioresource Technology, 366, 128189, 2022. https://doi.org/10.1016/j.biortech.2022.128189

[25] Wang, K., Kim, K. H., Brown, R. C. "Catalytic pyrolysis of individual components of lignocellulosic biomass", Green Chemistry, 16(2), pp. 727–735, 2014. https://doi.org/10.1039/c3gc41288a

[26] Dyer, A. C., Nahil, M. A., Williams, P. T. "Biomass:polystyrene co-pyrolysis coupled with metal-modified zeolite catalysis for liquid fuel and chemical production", Journal of Material Cycles and Waste Management, 24(2), pp. 477–490, 2022. https://doi.org/10.1007/s10163-021-01334-0

[27] Grams, J., Ruppert, A. M. "Development of Heterogeneous Catalysts for Thermo-Chemical Conversion of Lignocellulosic Biomass", Energies, 10(4), 545, 2017. https://doi.org/10.3390/en10040545

[28] Hernández-Giménez, A. M., Hernando, H., Danisi, R. M., Vogt, E. T. C., Houben, K., Baldus, M., Serrano, D. P., Bruijnincx, P. C. A., Weckhuysen, B. M. "Deactivation and regeneration of solid acid and base catalyst bodies used in cascade for bio-oil synthesis and upgrading", Journal of Catalysis, 405, pp. 641–651, 2022. https://doi.org/10.1016/j.jcat.2021.09.029

[29] Kabakcı, S. B., Hacıbektaşoğlu, Ş. "Catalytic Pyrolysis of Biomass", In: Samer, M. (ed.) Pyrolysis, IntechOpen, 2017, pp. 135–154. ISBN 978-953-51-3312-4 https://doi.org/10.5772/67569

[30] Mante, O. D., Agblevor, F. A., McClung, R. "A study on catalytic pyrolysis of biomass with Y-zeolite based FCC catalyst using response surface methodology", Fuel, 108, pp. 451–464, 2013. https://doi.org/10.1016/j.fuel.2012.12.027

[31] AlMohamadi, H., Aljabri, A., Mahmoud, E. R. I., Khan, S. Z., Aljohani, M. S., Shamsuddin, R. "Catalytic Pyrolysis of Municipal Solid Waste: Effects of Pyrolysis Parameters", Bulletin of Chemical Reaction Engineering & Catalysis, 16(2), pp. 342–352, 2021. https://doi.org/10.9767/bcrec.16.2.10499.342-352

[32] Rammohan, D., Kishore, N., Uppaluri, R. V. S. "Thermogravimetric analysis of pyrolysis of *Delonix regia* biomass in the presence of zeolite, mixed metal oxides and carbon supported noble metal catalysts", Results in Engineering, 17, 100936, 2023. https://doi.org/10.1016/j.rineng.2023.100936

[33] Singh, R., Chakinala, N., Mohanty, K., Chakinala, A. G. "Catalytic upgrading of biomass pyrolysis vapors for selective production of phenolic monomers over metal oxide modified alumina catalysts", Journal of Environmental Chemical Engineering, 11(6), 111518, 2023. https://doi.org/10.1016/j.jece.2023.111518

[34] Zhang, L., Bao, Z., Xia, S., Lu, Q., Walters, K. B. "Catalytic Pyrolysis of Biomass and Polymer Wastes", Catalysts, 8(12), 659, 2018. https://doi.org/10.3390/catal8120659

[35] Chen, X., Zhang, L., Wang, G., Zhao, X., Sun, S., …, Su, X. "Catalytic pyrolysis of waste biomass via coal fly ash for synergistic production of cost-effective artificial humic acid", Bioresource Technology, 442, 133682, 2026. https://doi.org/10.1016/j.biortech.2025.133682

[36] Zhang, X., Zhang, Y., Zhang, S., Yao, L., Hao, Y. "Lignocellulosic biomass pyrolysis: A review on the pretreatment and catalysts", Fuel Processing Technology, 279, 108352, 2025. https://doi.org/10.1016/j.fuproc.2025.108352

[37] Cheng, F., Li, X. "Preparation and Application of Biochar-Based Catalysts for Biofuel Production", Catalysts, 8(9), 346, 2018. https://doi.org/10.3390/catal8090346

[38] Li, P., Wan, K., Chen, H., Zheng, F., Zhang, Z., Niu, B., Zhang, Y., Long, D. "Value-Added Products from Catalytic Pyrolysis of Lignocellulosic Biomass and Waste Plastics over Biochar-Based Catalyst: A State-of-the-Art Review", Catalysts, 12(9), 1067, 2022. https://doi.org/10.3390/catal12091067

[39] ASTM International "ASTM E872-82(2019) Standard Test Method for Volatile Matter in the Analysis of Particulate Wood Fuels", ASTM International, West Conshohocken, PA, USA, 2019. https://doi.org/10.1520/E0872-82R19

[40] ASTM International "ASTM E1755-01(2020) Standard Test Method for Ash in Biomass", ASTM International, West Conshohocken, PA, USA, 2020. https://doi.org/10.1520/E1755-01R20

[41] ASTM International "ASTM E1756-01 Standard Test Method for Determination of Total Solids in Biomass", ASTM International, West Conshohocken, PA, USA, 2010. https://doi.org/10.1520/E1756-01

[42] ASTM International "ASTM D5373-02 Standard Test Methods for Instrumental Determination of Carbon, Hydrogen, and Nitrogen in Laboratory Samples of Coal and Coke", ASTM International, West Conshohocken, PA, USA, 2017. https://doi.org/10.1520/D5373-02

[43] TAPPI "TAPPI T 204 cm-17 Solvent Extractives of Wood and Pulp", Technical Association of the Pulp and Paper Industry, Peachtree Corners, GA, USA, 2017.

[44] TAPPI "TAPPI/ANSI T 222 om-21 Acid-Insoluble Lignin in Wood and Pulp", Technical Association of the Pulp and Paper Industry, Peachtree Corners, GA, USA, 2021.

[45] TAPPI "TAPPI T 203 cm-22 Alpha-, Beta- and Gamma-Cellulose in Pulp", Technical Association of the Pulp and Paper Industry, Peachtree Corners, GA, USA, 2022.

[46] ASTM International "ASTM D3172-13(2021)e1 Standard Practice for Proximate Analysis of Coal and Coke", ASTM International, West Conshohocken, PA, USA, 2021. https://doi.org/10.1520/D3172-13R21E01

[47] ASTM International "ASTM D3173/D3173M-25 Standard Test Method for Moisture in the Analysis Sample of Coal and Coke", ASTM International, West Conshohocken, PA, USA, 2025. https://doi.org/10.1520/D3173_D3173M-25

[48] ASTM International "ASTM D3174-12(2018)e1 Standard Test Method for Ash in the Analysis Sample of Coal and Coke from Coal", ASTM International, West Conshohocken, PA, USA, 2018. https://doi.org/10.1520/D3174-12R18E01

[49] ASTM International "ASTM D3175-26 Standard Test Method for Gross Calorific Value of Coal and Coke", ASTM International, West Conshohocken, PA, USA, 2026. https://doi.org/10.1520/D3175-26

[50] ASTM International "ASTM D5865/D5865M-19 Standard Test Method for Gross Calorific Value of Coal and Coke", ASTM International, West Conshohocken, PA, USA, 2019. https://doi.org/10.1520/D5865_D5865M-19

[51] ISO "ISO 6976:2016 Natural gas — Calculation of calorific values, density, relative density and Wobbe indices from composition", International Organization for Standardization, Geneva, Switzerland, 2016.

[52] GPA Midstream Association "GPA 2145:2016 Table of Physical Properties for Hydrocarbons and Other Compounds of Interest to the Natural Gas and Natural Gas Liquids Industries", GPA Midstream Association, Tulsa, OK, USA, 2016.

[53] Perry, R. H., Chilton, C. H. "Chemical Engineers' Handbook", McGraw-Hill Book Company, 1973. ISBN 0070855471

[54] Ahmad, M. S., Mehmood, M. A., Al Ayed, O. S., Ye, G., Luo, H., Ibrahim, M., Rashid, U., Arbi Nehdi, I., Qadir, G. "Kinetic analyses and pyrolytic behavior of Para grass (*Urochloa mutica*) for its bioenergy potential", Bioresource Technology, 224, pp. 708–713, 2017. https://doi.org/10.1016/j.biortech.2016.10.090

[55] Liu, H., Zhao, B., Zhang, X., Zhang, Y. "Influence of Intrinsic Physicochemical Properties of Agroforestry Waste on Its Pyrolysis Characteristics and Behavior", Materials, 16(1), 222, 2023. https://doi.org/10.3390/ma16010222

[56] Rezaei, H., Yazdanpanah, F., Choon Lim, J., Lau, A., Sokhansanj, S. "Woody Feedstock Pretreatments to Enhance Pyrolysis Bio-oil Quality and Produce Transportation Fuel", In: Abomohra, A. E.-F. (ed.) Biomass for Bioenergy - Recent Trends and Future Challenges, IntechOpen, 2019, pp. 1–20. ISBN 978-1-78923-988-1 https://doi.org/10.5772/intechopen.81818

[57] Allende, S., Brodie, G., Jacob, M. V. "Breakdown of biomass for energy applications using microwave pyrolysis: A technological review", Environmental Research, 226, 115619, 2023. https://doi.org/10.1016/j.envres.2023.115619

[58] Palamanit, A., Khongphakdi, P., Tirawanichakul, Y., Phusunti, N. "Investigation of yields and qualities of pyrolysis products obtained from oil palm biomass using an agitated bed pyrolysis reactor", Biofuel Research Journal, 6(4), pp. 1065–1079, 2019. https://doi.org/10.18331/BRJ2019.6.4.3

[59] Wang, Y., Li, B., Gao, A., Ding, K., Xing, X., Wei, J., Huang, Y., Chun-Ho Lam, J., Subramanian, K. A., Zhang, S. "Volatile-char interactions during biomass pyrolysis: Effect of biomass acid-washing pretreatment", Fuel, 340, 127496, 2023. https://doi.org/10.1016/j.fuel.2023.127496

[60] Tahir, M. H., Irfan, R. M., Hussain, M. B., Alhumade, H., Al-Turki, Y., Cheng, X., Karim, A., Ibrahim, M., Rathore, H. A. "Catalytic Fast Pyrolysis of Soybean Straw Biomass for Glycolaldehyde-Rich Bio-oil Production and Subsequent Extraction", ACS Omega, 6(49), pp. 33694–33700, 2021. https://doi.org/10.1021/acsomega.1c04717

[61] Shezi, M., Kiambi, S. L. "Isothermal Pyrolysis of Bamboo and Pinewood Biomass: Product Characterization and Comparative Study in a Fluidized Bed Reactor", Bioengineering, 12(2), 99, 2025. https://doi.org/10.3390/bioengineering12020099

[62] Venegas-Vásconez, D., Arteaga-Pérez, L. E., Aguayo, M. G., Romero-Carrillo, R., Guerrero, V. H., Tipanluisa-Sarchi, L., Alejandro-Martín, S. "Analytical Pyrolysis of *Pinus radiata* and *Eucalyptus globulus*: Effects of Microwave Pretreatment on Pyrolytic Vapours Composition", Polymers, 15(18), 3790, 2023. https://doi.org/10.3390/polym15183790

[63] Zhao, C., Jiang, E., Chen, A. "Volatile production from pyrolysis of cellulose, hemicellulose and lignin", Journal of the Energy Institute, 90(6), pp. 902–913, 2017. https://doi.org/10.1016/j.joei.2016.08.004

[64] Chen, D., Cen, K., Zhuang, X., Gan, Z., Zhou, J., Zhang, Y., Zhang, H. "Insight into biomass pyrolysis mechanism based on cellulose, hemicellulose, and lignin: Evolution of volatiles and kinetics, elucidation of reaction pathways, and characterization of gas, biochar and bio-oil", Combustion and Flame, 242, 112142, 2022. https://doi.org/10.1016/j.combustflame.2022.112142

[65] Mammadova, T., Ahmadova, G., Karimli, R. "Thermochemical Conversion of Beech Wood Residues in a Fixed-Bed Reactor: Product Yields and Quality Analysis under Varying Pyrolysis Temperatures", Egyptian Journal of Petroleum, 35(2), 10, 2026. https://doi.org/10.62593/2090-2468.1112

[66] Saidi, M., Zhandnezhad, A. "Valorization of neem seeds biomass to biofuel via non-catalytic and catalytic pyrolysis process: Investigation of catalytic activity of Co–Mo/Al_2O_3 and Ni–Mo/Al_2O_3 for biofuel production", Journal of Environmental Management, 326, 116761, 2023. https://doi.org/10.1016/j.jenvman.2022.116761

[67] Ren, J., Cao, J.-P., Zhao, X.-Y., Liu, Y.-L. "Recent progress and perspectives of catalyst design and downstream integration in biomass tar reforming", Chemical Engineering Journal, 429, 132316, 2022. https://doi.org/10.1016/j.cej.2021.132316

[68] Wicakso, D. R., Nurandini, D., Mirwan, A., Putra, M. D. "Integration of pyrolysis – tar decomposition over porous low grade iron ore", IOP Conference Series: Materials Science and Engineering, 722(1), 012053, 2020. https://doi.org/10.1088/1757-899X/722/1/012053

[69] Zhang, Y., Chen, G., Wang, L., Tuo, K., Liu, S. "Microwave-Assisted Pyrolysis of Low-Rank Coal with K_2CO_3, $CaCl_2$, and $FeSO_4$ Catalysts", ACS Omega, 5(28), pp. 17232–17241, 2020. https://doi.org/10.1021/acsomega.0c01400

[70] Lugovoy, Y. V., Chalov, K. V., Kosivtsov, Y. Y., Stepacheva, A. A., Sulman, E. M. "A study of fast pyrolysis of plant biomass assisted by the conversion of volatile products using Fe(Co, Ni)/ZSM-5 catalysts", Catalysis for Sustainable Energy, 7(1), pp. 37–44, 2020. https://doi.org/10.1515/cse-2020-0004

[71] Chai, Y., Wang, M., Gao, N., Duan, Y., Li, J. "Experimental study on pyrolysis/gasification of biomass and plastics for H2 production under new dual-support catalyst", Chemical Engineering Journal, 396, 125260, 2020. https://doi.org/10.1016/j.cej.2020.125260

[72] Ismail, T. M., Banks, S. W., Yang, Y., Yang, H., Chen, Y., Bridgwater, A. V., Ramzy, K., Abd El-Salam, M. "Coal and biomass co-pyrolysis in a fluidized-bed reactor: Numerical assessment of fuel type and blending conditions", Fuel, 275, 118004, 2020. https://doi.org/10.1016/j.fuel.2020.118004

[73] Hu, M., Cui, B., Xiao, B., Luo, S., Guo, D. "Insight into the Ex Situ Catalytic Pyrolysis of Biomass over Char Supported Metals Catalyst: Syngas Production and Tar Decomposition", Nanomaterials, 10(7), 1397, 2020. https://doi.org/10.3390/nano10071397

[74] Lan, K., Shang, S., Guo, C., Xiong, T., Qin, Z., He, W., Li, J. "Preparation of fly ash nickel catalyst and its application in catalytic pyrolysis of rice straw for syngas production", BioResources, 14(3), pp. 6983–7000, 2019. https://doi.org/10.15376/biores.14.3.6983-7000

[75] Chou, C.-Y., Loiland, J. A., Lobo, R. F. "Reverse Water-Gas Shift Iron Catalyst Derived from Magnetite", Catalysts, 9(9), 773, 2019. https://doi.org/10.3390/catal9090773

[76] Díaz-Verde, Á., Montilla-Verdú, S., Torregrosa-Rivero, V., Illán-Gómez, M.-J. "Tailoring the Composition of Ba_xBO_3 (B = Fe, Mn) Mixed Oxides as CO or Soot Oxidation Catalysts in Simulated GDI Engine Exhaust Conditions", Molecules, 28(8), 3327, 2023. https://doi.org/10.3390/molecules28083327

[77] Han, S. J., Hwang, S.-M., Park, H.-G., Zhang, C., Jun, K.-W., Kim, S. K. "Identification of active sites for CO_2 hydrogenation in Fe catalysts by first-principles microkinetic modelling", Journal of Materials Chemistry A, 8(26), pp. 13014–13023, 2020. https://doi.org/10.1039/d0ta01634a

[78] Lv, X., Ma, Y., Li, Y., Yang, Q. "Heterogeneous Fenton-Like Catalytic Degradation of 2,4-Dichlorophenoxyacetic Acid by Nano-Scale Zero-Valent Iron Assembled on Magnetite Nanoparticles", Water, 12(10), 2909, 2020. https://doi.org/10.3390/w12102909

[79] Sun, T., Li, Z., Zhang, Z., Wang, Z., Yang, S., Yang, Y., Wang, X., Liu, S., Zhang, Q., Lei, T. "Fast corn stalk pyrolysis and the influence of catalysts on product distribution", Bioresource Technology, 301, 122739, 2020. https://doi.org/10.1016/j.biortech.2020.122739

[80] Wicakso, D. R., Sutijan, S., Rochmadi, R., Hidayat, M., Cahyono, R. B., Budiman A. "Effect of Temperature on Catalytic Decomposition of Tar using Indonesian Iron Ore as Catalyst", International Journal of Renewable Energy Research, 8(1), pp. 421–427, 2018.
https://doi.org/10.20508/ijrer.v8i1.6870.g7317

[81] Aliyu, A., Lee, J. G. M., Harvey, A. P. "Microalgae for biofuel: Comparing the performance of solvent-free sulfated zirconia catalysts and zeolite Y for the catalytic pyrolysis of freshwater microalgae (*Chlorella vulgaris*)", Next Sustainability, 5, 100141, 2025.
https://doi.org/10.1016/j.nxsust.2025.100141

[82] Hafriz, R. S. R. M., Arifin, N. A., Salmiaton, A., Yunus, R., Taufiq-Yap, Y. H., Saifuddin, N. M., Shamsuddin, A. H. "Multiple-objective optimization in green fuel production via catalytic deoxygenation reaction with NiO-dolomite catalyst", Fuel, 308, 122041, 2022.
https://doi.org/10.1016/j.fuel.2021.122041

[83] Ma, H., Hu, Y., Zhu, H., Jiang, Q., Chen, T. "Contrasting Catalytic Pathways in Lignin Pyrolysis: Deoxygenative Cracking over HZSM-5 Versus Repolymerization–Coking over Activated Carbon", Polymers, 18(3), 408, 2026.
https://doi.org/10.3390/polym18030408

[84] Jin, T., Wang, H., Peng, J., Wu, Y., Huang, Z., Tian, X., Ding, M. "Catalytic pyrolysis of lignin with metal-modified HZSM-5 as catalysts for monocyclic aromatic hydrocarbons production", Fuel Processing Technology, 230, 107201, 2022.
https://doi.org/10.1016/j.fuproc.2022.107201

[85] Puértolas, B., Veses, A., Callén, M. S., Mitchell, S., García, T., Pérez-Ramírez, J. "Porosity–Acidity Interplay in Hierarchical ZSM-5 Zeolites for Pyrolysis Oil Valorization to Aromatics", ChemSusChem, 8(19), pp. 3283–3293, 2015.
https://doi.org/10.1002/cssc.201500685

[86] Nurhadi, N., Rianda, S., Irawan, C., Pramono, G. P. "Biochar production investigation from pyrolysis of lamtoro wood as a coal blend for fuel substitution in steam power plants", IOP Conference Series: Earth and Environmental Science, 749(1), 012037, 2021.
https://doi.org/10.1088/1755-1315/749/1/012037

[87] Nath, B., Chen, G., Bowtell, L., Nguyen-Huy, T. "Pyrolysis of wheat straw pellets in a pilot-scale reactor: Effect of temperature and residence time", Energy Science & Engineering, 12(8), pp. 3524–3539, 2024.
https://doi.org/10.1002/ese3.1833

[88] Cheng, J., Hu, S.-C., Sun, G.-T., Geng, Z.-C., Zhu, M.-Q. "The effect of pyrolysis temperature on the characteristics of biochar, pyroligneous acids, and gas prepared from cotton stalk through a polygeneration process", Industrial Crops and Products, 170, 113690, 2021.
https://doi.org/10.1016/j.indcrop.2021.113690

[89] Fawzy, S., Osman, A. I., Yang, H., Doran, J., Rooney, D. W. "Industrial biochar systems for atmospheric carbon removal: a review", Environmental Chemistry Letters, 19(4), pp. 3023–3055, 2021.
https://doi.org/10.1007/s10311-021-01210-1

[90] Tomczyk, A., Sokołowska, Z., Boguta, P. "Biochar physicochemical properties: pyrolysis temperature and feedstock kind effects", Reviews in Environmental Science and Bio/Technology, 19(1), pp. 191–215, 2020.
https://doi.org/10.1007/s11157-020-09523-3

[91] Wystalska, K., Kwarciak-Kozłowska, A. "The Effect of Biodegradable Waste Pyrolysis Temperatures on Selected Biochar Properties", Materials, 14(7), 1644, 2021.
https://doi.org/10.3390/ma14071644

[92] Ravindiran, G., Rajamanickam, S., Janardhan, G., Hayder, G., Alagumalai, A., Mahian, O., Lam, S. S., Sonne, C. "Production and modifications of biochar to engineered materials and its application for environmental sustainability: a review", Biochar, 6(1), 62, 2024.
https://doi.org/10.1007/s42773-024-00350-1